buffer), before being stained with a PE- or APC-conjugated anti-mouse IFN-γ mAb (clone XMG1.2; eBioscience) or isotype control Ab (eBioscience) for 45 min at 4 °C. Cells were washed, first with permeabilization buffer, then with FACS buffer, before being applied to a FACSCalibur or FACSAria flow cytometer (BD). Analyses were performed using FlowJo software (Ashland, OR).

Cytological analysis. Fifty thousand cells were subjected to a cytospin (Thermo Shandon). For morphological analysis, the cytospin preparations were fixed with methanol and visualized with May-Grünwald-Giemsa staining. For intracellular IFN-γ staining, the cytospin preparations were fixed with 2% paraformaldehyde for 10 min, treated with 50 mM NH_4Cl/PBS for 15 min, and blocked with an anti-mouse FcγR mAb (clone 2.4G2) in permeabilization buffer for 15 min. Slides were stained with an APC-conjugated anti-mouse IFN-γ mAb (clone XMG1.2) or isotype control Ab (eBioscience) for 45 min, washed 3 times with permeabilization buffer, and then washed 3 times with PBS. Nuclei were visualized with propidium iodide staining. Samples were viewed and photographed with a Carl Zeiss LSM510 confocal laser scanning microscope.

Histology. For histological analysis, the tissues from GAS-infected mice were fixed in 10% formalin/PBS. The paraffin-embedded sections were stained with hematoxylin and eosin.

***In vitro* culture of γIMCs and BMPCs**. Purified CD11b$^+$ CD11c$^-$ F4/80^{low} Ly-6G$^+$ γIMCs and CD11b$^+$ CD11c^{low} F4/80$^+$ Ly-6G^{low} BMPCs from GAS-infected (monensin-untreated) mice were cultured at 0.5×10^6 cells per ml in medium containing RPMI 1640 (Wako) with 10% FBS (Nichirei), 100 U ml^{-1} penicillin, 10 μg ml^{-1} streptomycin, 2 mM glutamine, 25 mM HEPES, and 50 μM 2-ME, with or without 10–50 ng ml^{-1} recombinant mouse GM-CSF, G-CSF, M-CSF, or IL-5 (R&D Systems), in the presence or absence of 1 μg ml^{-1} control rat IgG or R4-6A2, for 2–6 days. On days 2 and 4, 50% of the medium was replaced with fresh medium, or the cells were collected for May-Grünwald-Giemsa staining and flow cytometry analysis. In some experiments, the cells were cultured at 0.5×10^6 cells ml^{-1} with 25 μg ml^{-1} erythromycin and NIH34 (MOI 100) in 10% FBS/phenol red-free RPMI medium, supplemented with 10 ng ml^{-1} GM-CSF, in the presence of 1 μg ml^{-1} control rat IgG or R4-6A2 for 24 h. The levels of IFN-γ and NO in the culture supernatants were measured by an instant ELISA kit (eBioscience) and a Griess reagent (Wako), respectively, according to the manufacturer's instructions.

***In vitro* culture of Eos and MDSCs**. For obtaining Eos, naïve bone marrow cells were cultured in 10% FBS/RPMI medium supplemented with stem cell factor (PeproTech) and FLT3-ligand (PeproTech) for 4 days, and then with medium containing recombinant mouse IL-5 (R&D Systems). On day 12, the cells were collected for May-Grünwald-Giemsa staining and flow cytometry analysis[46]. To isolate bone marrow-derived MDSCs, naïve bone marrow cells were cultured at 1.0×10^6 cells per ml in 10% FBS/RPMI medium, supplemented with 40 ng ml^{-1} GM-CSF. On day 4, the cells were collected for FACS analysis of CD11b$^+$ CD11c$^-$ Ly-6C$^+$ Ly-6G^{low} MDSCs[9].

Ag-specific T-cell proliferation and IFN-γ production. The Ag-specific proliferation of CD8$^+$ T cells was evaluated using OT-I OVA-specific MHC Class I-restricted TCR transgenic mice. Varying amounts of purified CD11b$^+$ CD11c$^-$ F4/80^{low} Ly-6G$^+$ γIMCs from infected C57BL/6 mice at 2 days post-infection, or bone marrow-derived F4/80$^+$ Ly-6C$^+$ Ly-6G^{low} MDSCs, were added to 2.0×10^5 naïve splenocytes from OT-I mice in medium containing RPMI 1640 with 10% FBS in a U-bottom 96-well plate. These co-cultures were stimulated with antigenic $OVA_{357-364}$ peptides (10 μM) for 4 days. Proliferation of OT-I cells in triplicate was estimated by the incorporation of [^{3}H] thymidine (1 μCi (0.0037 MBq) per well), added at 18 h before cell harvest. The level of IFN-γ in the culture supernatants was measured by an instant ELISA kit (eBioscience), according to the manufacturer's instructions.

Adoptive transfer of γIMCs. CD11b$^+$ CD11c$^-$ F4/80^{low} Ly-6G$^+$ γIMCs in splenocytes from *Ifng*$^{+/+}$ mice infected with NIH34 (3.0×10^7 CFU) for 48 h were isolated with a FACSAria flow cytometer. Recipient mice were i.v. administered with purified CD11b$^+$ CD11c$^-$ F4/80^{low} Ly-6G$^+$ γIMCs (3.0×10^6 cells), and i.p. inoculated with NIH34 (1.0×10^7 CFU to 5.0×10^7 CFU) on the same day.

Measurement of bacterial loads. At 24 h post-infection, 20 μl of peripheral blood was removed from the tail vein by phlebotomy. The blood was diluted at 1:10–1:1000 with PBS and spread on a Columbia agar plate containing 5% sheep blood (BD). To determine the number of NIH34 in peripheral blood, the plates were incubated for 20 h at 37 °C in a 5% CO_2 atmosphere, and the colonies were counted. The number of NIH34 was compared statistically using the Mann–Whitney *U*-test.

References

1. Lappin, E. & Ferguson, A. J. Gram-positive toxic shock syndromes. *Lancet Infect. Dis.* **9,** 281–290 (2009).
2. Cunningham, M. W. Pathogenesis of group A streptococcal infections. *Clin. Microbiol. Rev.* **13,** 470–511 (2000).
3. Davies, H. D *et al.* Invasive group A streptococcal infections in Ontario, Canada. Ontario Group A Streptococcal Study Group. *N. Engl. J. Med.* **335,** 547–554 (1996).
4. Bisno, A. L. & Stevens, D. L. Streptococcal infections of skin and soft tissues. *N. Engl. J. Med.* **334,** 240–245 (1996).
5. Raeder, R. H., Barker-Merrill, L., Lester, T., Boyle, M. D. & Metzger, D. W. A pivotal role for interferon-gamma in protection against group A streptococcal skin infection. *J. Infect. Dis.* **181,** 639–645 (2000).
6. Stavem, P., Hjort, P. F., Vogt, E. & van der Hagen, C. B. Ring-shaped nuclei of granulocytes in a patient with acute erythroleukaemia. *Scand. J. Haematol.* **6,** 31–32 (1969).
7. Langenhuijsen, M. M. Neutrophils with ring-shaped nuclei in myeloproliferative disease. *Br. J. Haematol.* **58,** 227–230 (1984).
8. Biermann, H. *et al.* Murine leukocytes with ring-shaped nuclei include granulocytes, monocytes, and their precursors. *J. Leukoc. Biol.* **65,** 217–231 (1999).
9. Rossner, S. *et al.* Myeloid dendritic cell precursors generated from bone marrow suppress T cell responses via cell contact and nitric oxide production *in vitro*. *Eur. J. Immunol.* **35,** 3533–3544 (2005).
10. Dardalhon, V. *et al.* Tim-3/galectin-9 pathway: regulation of Th1 immunity through promotion of CD11b+Ly-6G+ myeloid cells. *J. Immunol.* **185,** 1383–1392 (2010).
11. Movahedi, K. *et al.* Identification of discrete tumor-induced myeloid-derived suppressor cell subpopulations with distinct T cell-suppressive activity. *Blood* **111,** 4233–4244 (2008).
12. Youn, J. I., Nagaraj, S., Collazo, M. & Gabrilovich, D. I. Subsets of myeloid-derived suppressor cells in tumor-bearing mice. *J. Immunol.* **181,** 5791–5802 (2008).
13. Ribechini, E., Greifenberg, V., Sandwick, S. & Lutz, M. B. Subsets, expansion and activation of myeloid-derived suppressor cells. *Med. Microbiol. Immunol.* **199,** 273–281 (2010).
14. Medina, E., Goldmann, O., Rohde, M., Lengeling, A. & Chhatwal, G. S. Genetic control of susceptibility to group A streptococcal infection in mice. *J. Infect. Dis.* **184,** 846–852 (2001).
15. Goldmann, O., Chhatwal, G. S. & Medina, E. Immune mechanisms underlying host susceptibility to infection with group A streptococci. *J. Infect. Dis.* **187,** 854–861 (2003).
16. Goldmann, O. *et al.* The role of the MHC on resistance to group a streptococci in mice. *J. Immunol.* **175,** 3862–3872 (2005).
17. Goldmann, O., Chhatwal, G. S. & Medina, E. Contribution of natural killer cells to the pathogenesis of septic shock induced by Streptococcus pyogenes in mice. *J. Infect. Dis.* **191,** 1280–1286 (2005).
18. Ikebe, T. *et al.* Highly frequent mutations in negative regulators of multiple virulence genes in group A streptococcal toxic shock syndrome isolates. *PLoS Pathog.* **6,** e1000832 (2010).
19. Arad, G., Levy, R., Hillman, D. & Kaempfer, R. Superantigen antagonist protects against lethal shock and defines a new domain for T-cell activation. *Nat. Med.* **6,** 414–421 (2000).
20. Norrby-Teglund, A. *et al.* Evidence for superantigen involvement in severe group a streptococcal tissue infections. *J. Infect. Dis.* **184,** 853–860 (2001).
21. Kotb, M. *et al.* An immunogenetic and molecular basis for differences in outcomes of invasive group A streptococcal infections. *Nat. Med.* **8,** 1398–1404 (2002).
22. Liu, F. & Whitton, J. L. Cutting edge: re-evaluating the *in vivo* cytokine responses of CD8+ T cells during primary and secondary viral infections. *J. Immunol.* **174,** 5936–5940 (2005).
23. Sun, J., Madan, R., Karp, C. L. & Braciale, T. J. Effector T cells control lung inflammation during acute influenza virus infection by producing IL-10. *Nat. Med.* **15,** 277–284 (2009).
24. Nooh, M. M., El-Gengehi, N., Kansal, R., David, C. S. & Kotb, M. HLA transgenic mice provide evidence for a direct and dominant role of HLA class II variation in modulating the severity of streptococcal sepsis. *J. Immunol.* **178,** 3076–3083 (2007).
25. Abdeltawab, N. F. *et al.* An unbiased systems genetics approach to mapping genetic loci modulating susceptibility to severe streptococcal sepsis. *PLoS Pathog.* **4,** e1000042 (2008).
26. Mombaerts, P. *et al.* RAG-1-deficient mice have no mature B and T lymphocytes. *Cell* **68,** 869–877 (1992).
27. Ato, M., Ikebe, T., Kawabata, H., Takemori, T. & Watanabe, H. Incompetence of neutrophils to invasive group A streptococcus is attributed to induction of plural virulence factors by dysfunction of a regulator. *PLoS One* **3,** e3455 (2008).
28. Eriksson, B. K., Andersson, J., Holm, S. E. & Norgren, M. Epidemiological and clinical aspects of invasive group A streptococcal infections and the streptococcal toxic shock syndrome. *Clin. Infect. Dis.* **27,** 1428–1436 (1998).
29. Iwasaki, H. *et al.* Identification of eosinophil lineage-committed progenitors in the murine bone marrow. *J. Exp. Med.* **201,** 1891–1897 (2005).

30. Angulo, I. *et al.* Involvement of nitric oxide in bone marrow-derived natural suppressor activity. Its dependence on IFN-gamma. *J. Immunol.* **155,** 15–26 (1995).
31. Angulo, I. *et al.* Early myeloid cells are high producers of nitric oxide upon CD40 plus IFN-gamma stimulation through a mechanism dependent on endogenous TNF-alpha and IL-1alpha. *Eur. J. Immunol.* **30,** 1263–1271 (2000).
32. Pelaez, B., Campillo, J. A., Lopez-Asenjo, J. A. & Subiza, J. L. Cyclophosphamide induces the development of early myeloid cells suppressing tumor cell growth by a nitric oxide-dependent mechanism. *J. Immunol.* **166,** 6608–6615 (2001).
33. Campillo, J. A., Pelaez, B., Angulo, I., Bensussan, A. & Subiza, J. L. Involvement of IFNbeta on IFNgamma and nitric oxide (NO) production by bone marrow (BM) cells in response to lipopolysaccharide. *Biomed. Pharmacother.* **60,** 541–547 (2006).
34. Gallina, G. *et al.* Tumors induce a subset of inflammatory monocytes with immunosuppressive activity on CD8+ T cells. *J. Clin. Invest.* **116,** 2777–2790 (2006).
35. Belyaev, N. N. *et al.* Induction of an IL7-R(+)c-Kit(hi) myelolymphoid progenitor critically dependent on IFN-gamma signaling during acute malaria. *Nat. Immunol.* **11,** 477–485 (2010).
36. Serbina, N. V., Jia, T., Hohl, T. M. & Pamer, E. G. Monocyte-mediated defense against microbial pathogens. *Annu. Rev. Immunol.* **26,** 421–452 (2008).
37. Metcalf, D. & Nicola, N. A. Proliferative effects of purified granulocyte colony-stimulating factor (G-CSF) on normal mouse hemopoietic cells. *J. Cell. Physiol.* **116,** 198–206 (1983).
38. Hitoshi, Y. *et al.* Distribution of IL-5 receptor-positive B cells. Expression of IL-5 receptor on Ly-1(CD5)+ B cells. *J. Immunol.* **144,** 4218–4225 (1990).
39. Lee, J. J. & McGarry, M. P. When is a mouse basophil not a basophil? *Blood* **109,** 859–861 (2007).
40. Delano, M. J. *et al.* MyD88-dependent expansion of an immature GR-1(+) CD11b(+) population induces T cell suppression and Th2 polarization in sepsis. *J. Exp. Med.* **204,** 1463–1474 (2007).
41. Zhan, Y., Lieschke, G. J., Grail, D., Dunn, A. R. & Cheers, C. Essential roles for granulocyte-macrophage colony-stimulating factor (GM-CSF) and G-CSF in the sustained hematopoietic response of Listeria monocytogenes-infected mice. *Blood* **91,** 863–869 (1998).
42. Baldridge, M. T., King, K. Y., Boles, N. C., Weksberg, D. C. & Goodell, M. A. Quiescent haematopoietic stem cells are activated by IFN-gamma in response to chronic infection. *Nature* **465,** 793–797 (2010).
43. Trottier, M. D., Newsted, M. M., King, L. E. & Fraker, P. J. Natural glucocorticoids induce expansion of all developmental stages of murine bone marrow granulocytes without inhibiting function. *Proc. Natl Acad. Sci. USA* **105,** 2028–2033 (2008).
44. Breiman, R. F. *et al.* Defining the group A streptococcal toxic shock syndrome. Rationale and consensus definition. *JAMA* **269,** 390–391 (1993).
45. Dalton, D. K. *et al.* Multiple defects of immune cell function in mice with disrupted interferon-gamma genes. *Science* **259,** 1739–1742 (1993).
46. Dyer, K. D. *et al.* Functionally competent eosinophils differentiated *ex vivo* in high purity from normal mouse bone marrow. *J. Immunol.* **181,** 4004–4009 (2008).

Acknowledgements

We thank Dr. Satoshi Takaki (Research Institute National Center for Global Health and Medicine) and Dr. Kiyoshi Takatsu (University of Toyama) for providing the anti-IL-5Rα mAb (clone H7); Dr. Akihiko Yoshimura (Keio University) for providing the anti-IFN-γ mAb; Dr. Hideki Fujii and Dr. Shigeo Koyasu (Keio University) for providing the OT-I transgenic mice; Dr. Paul M. Kaye (University of York) for critical comments; and Ms Yoko Nakamura for technical assistance. This work was partly supported by a grant (H22-Shinkou-Ippan-013 to M.A., T.I., and H.W.) from the Ministry of Health, Labour and Welfare of Japan, and by a Grant-in-Aid for Young Scientists (B) (22790959 to T.M.) from the Japan Society for the Promotion of Science.

Author contributions

T.M., M.A., and T.I. designed and performed the experiments. T.M. and M.A. analysed the data. T.M., M.A., T.I., M.O., H.W. and K.K. wrote the manuscript.

Additional information

Supplementary Information accompanies this paper at http://www.nature.com/naturecommunications

Competing financial interests: The authors declare no competing financial interests.

Reprints and permission information is available online at http://npg.nature.com/reprintsandpermissions/

How to cite this article: Matsumura, T. *et al.* Interferon-γ-producing immature myeloid cells confer protection against severe invasive group A *Streptococcus* infections *Nat. Commun.* 3:678 doi: 10.1038/ncomms1677 (2012).

Memory B cells in the lung participate in protective humoral immune responses to pulmonary influenza virus reinfection

Taishi Onodera[a], Yoshimasa Takahashi[a,1], Yusuke Yokoi[a,b], Manabu Ato[a], Yuichi Kodama[a], Satoshi Hachimura[b], Tomohiro Kurosaki[c,d], and Kazuo Kobayashi[a]

[a]Department of Immunology, National Institute of Infectious Diseases, Shinjuku-ku, Tokyo 162-8640, Japan; [b]Research Center for Food Safety, Graduate School of Agricultural and Life Sciences, University of Tokyo, Bunkyo-ku, Tokyo 113-8657, Japan; [c]Laboratory of Lymphocyte Differentiation, World Premier International Immunology Frontier Research Center, and Graduate School of Frontier Biosciences, Osaka University, Suita, Osaka 565-0871, Japan; and [d]Laboratory for Lymphocyte Differentiation, RIKEN Research Center for Allergy and Immunology, Tsurumi-ku, Yokohama, Kanagawa 230-0045, Japan

Edited* by Michel C. Nussenzweig, The Rockefeller University, New York, NY, and approved December 29, 2011 (received for review September 18, 2011)

After pulmonary virus infection, virus-binding B cells ectopically accumulate in the lung. However, their contribution to protective immunity against reinfecting viruses remains unknown. Here, we show the phenotypes and protective functions of virus-binding memory B cells that persist in the lung following pulmonary infection with influenza virus. A fraction of virus-binding B-cell population in the lung expressed surface markers for splenic mature memory B cells (CD73, CD80, and CD273) along with CD69 and CXCR3 that are up-regulated on lung effector/memory T cells. The lung B-cell population with memory phenotype persisted for more than 5 mo after infection, and on reinfection promptly differentiated into plasma cells that produced virus-neutralizing antibodies locally. This production of local IgG and IgA neutralizing antibody was correlated with reduced virus spread in adapted hosts. Our data demonstrates that infected lungs harbor a memory B-cell subset with distinctive phenotype and ability to provide protection against pulmonary virus reinfection.

lung memory B cells | viral immunity

B-cell memory is bipartite, consisting of both long-lived plasma cells and memory B cells. Immediate protection against reinfection is mediated by long-lived plasma cells that are present in the bone marrow and secrete antibodies in an antigen-independent fashion. Recall responses are mediated by memory B cells that rapidly proliferate and differentiate in response to antigenic stimulation (1, 2). The accessibility of memory B cells to reinfecting pathogens is, therefore, likely a significant factor in determining the effectiveness of humoral protection against reinfection. Thus, it is fundamentally important to determine the protective functions of pathogen-specific memory B cells that reside at the sites of infection after the resolution of a primary infection.

In the case of influenza virus, the initial infection and replication occur in the respiratory tract. These elicit immune responses in associated secondary lymphoid organs, e.g., mediastinal lymph nodes (MLNs), which support the initial rounds of B-cell priming that follow a pulmonary infection (3). In addition, nonlymphoid organs, including the lungs, participate in these primary responses. Indeed, after primary infection with influenza virus, infected lungs often support the development of ectopic tertiary lymphoid structures known as induced bronchus-associated lymphoid tissue (iBALT) that contain germinal centers (GCs) and plasma cells (4). Moreover, infected lungs harbor the precursors of virus-binding plasma cells as revealed after in vitro stimulation of lung cells (5, 6), suggesting the existence of virus-binding memory B cells in the lungs. However, virus-binding memory B cells in the lungs have not been indentified at cellular level, thereby their phenotypic and functional characterization is still lacking.

In this study, we characterized the phenotypes and functions of class-switched, influenza-specific B cells in the lungs. We show that a fraction of class-switched, influenza-specific B cells in the lungs possess a memory phenotype, persist for a long period, and respond to virus reinfection by promoting rapid viral clearance. Our data demonstrate that local tissues are important sites for the maintenance and reactivation of protective humoral memory responses.

Results

Infection with Influenza Virus Induces Antigen-Specific Memory-Like B-Cell Population in Lung. Pulmonary infection with influenza viruses induces precursors of antigen-specific, class-switched plasma cells in the lungs (5, 6); however, the phenotypes of these cells have not been determined. To characterize the phenotype and persistence of influenza-specific B cells in lungs, we labeled B cells recovered from lung tissue with recombinant hemagglutinin (rHA) conjugated to PE. Non-B cells, transitional B cells, B1 cells, and plasma cells were excluded from our analyses by colabeling with 12 mAbs specific for their surface markers (*SI Materials and Methods* and Fig. S1). IgM/D$^+$ cells were also excluded from the present analysis to reduce the risk of including naïve HA-binding B cells present in the preimmune repertoire (7). This staining procedure resulted in the clear visualization of HA-binding, class-switched B cells in mice infected with the X31 influenza virus but not with other influenza virus subtypes (Fig. S1), confirming our methods' specificity and sensitivity. Among the HA-binding IgM/D$^-$ lung B cells was a CD38$^+$ subset that could represent a memory B-cell population (8, 9). We first traced the numbers of both CD38$^+$ and CD38$^-$ B cells in lung, MLN, and spleen for 160 d after a primary infection (Fig. 1 *A* and *B*). The numbers of HA-binding IgM/D$^-$CD38$^-$ B cells rapidly but transiently increased in lung, MLN, and spleen. However, CD38$^-$ B cells in MLNs persisted for a longer period than those in lungs and spleens, similar to splenic or MLN GCs following vesicular stomatitis or influenza virus infection, respectively (10, 11).

HA-binding IgM/D$^-$CD38$^+$ B cells were found in the lung, MLN, and spleen, but lung CD38$^+$ B cells required more time to reach equilibrium than that required for CD38$^+$ B cells in other organs (Fig. 1*B*). This process resembles the slower accumulation of plasma cells in the lungs after influenza virus infection (11) and may reflect a requirement for structural alteration and/or niche formation in the infected lungs for B-cell localization.

Author contributions: Y.T., M.A., S.H., T.K., and K.K. designed research; T.O., Y.T., Y.Y., and Y.K. performed research; T.O. and Y.T. analyzed data; and Y.T., T.K., and K.K. wrote the paper.

The authors declare no conflict of interest.

*This Direct Submission article had a prearranged editor.

[1]To whom correspondence should be addressed. E-mail: ytakahas@nih.go.jp.

This article contains supporting information online at www.pnas.org/lookup/suppl/doi:10.1073/pnas.1115369109/-/DCSupplemental.

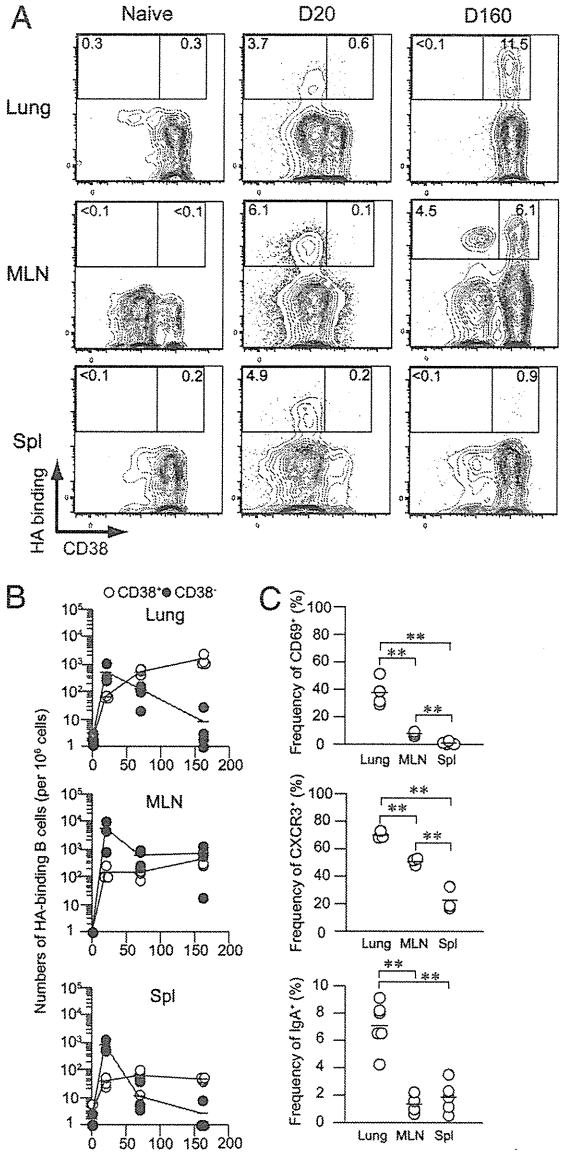

Fig. 1. Kinetics and surface phenotypes of HA-binding IgM/D$^-$ B-cell populations. (*A*) Cells recovered at the indicated time points after infection were subjected to flow-cytometric analysis (n = 4–5). Representative flow data for HA-binding/CD38 expression by IgM/D$^-$dump$^-$ B cells (Fig. S1) are shown. (*B*) Absolute cell number of CD38$^+$ and CD38$^-$ cells within the lymphocyte gate was plotted. (*C*) The frequencies of cells expressing CD69, CXCR3, or IgA are plotted. In *B* and *C*, each circle represents the result for an individual mouse (lung and spleen) and two to four pooled mice (MLN). $^{**}P < 0.01$.

Once generated, HA-binding IgM/D$^-$CD38$^+$ B cells stably persisted for 160 d after infection in all organs.

Although definitive markers of murine memory B cells remain to be identified (12, 13), CD73, CD80, and CD273 (PD-L2) are expressed at higher levels on splenic memory than on naïve B cells (14, 15). It is also postulated that the proportions of CD80$^+$ and/or CD273$^+$ cells reflect the maturation of memory B cells, because CD80$^+$ and/or CD273$^+$ cells express isotype-switched, somatically mutated B cell receptors more frequently than CD80$^-$CD273$^-$ cells (15). HA-binding IgM/D$^-$CD38$^+$ B cells in the lung, MLN, and spleen expressed increased levels of CD73, CD80, and CD273 than naïve B cells (IgD$^+$CD38$^+$B220$^+$) from the same tissue (Fig. S2). The phenotypic similarity of these HA-binding B cells to hapten-binding memory B cells (14, 15) supports our hypothesis that HA-binding IgM/D$^-$CD38$^+$ B cells represent a memory population. Significantly, HA-binding IgM/D$^-$CD38$^+$ lung B cells expressed CD73, CD80, and CD273 at higher frequencies than comparable populations in the MLN and spleen (Fig. S2); however, CD80 expression in the lung and MLN did not differ significantly. Considering the slow and steady accumulation of HA-binding IgM/D$^-$CD38$^+$ lung B cells, they may suggest that these lung B cells develop after progressive acquisition of mature memory phenotypes.

Further characterization revealed distinctive features of HA-binding IgM/D$^-$CD38$^+$ lung B cells. These lung B cells showed elevated expression of CD69 and CXCR3, a chemokine receptor governing effector T-cell migration to inflamed lung tissue (16), compared with the comparable populations in MLN and spleen (Fig. 1*C* and Fig. S3). Notably, Lee et al. (17) recently suggested that CD69 regulates lung localization of CD8$^+$ T cells following influenza virus infection. Thus, HA-binding IgM/D$^-$CD38$^+$ lung B cells expressed elevated levels of localization factors that direct the infiltration and residence of T cells in response to lung inflammation; however, the contribution of these to lung B-cell localization is not yet known. Together, phenotypic characterization of HA-binding IgM/D$^-$CD38$^+$ lung B cells revealed their unique phenotypes sharing surface markers for murine memory B cells with lung localization factors. Hereafter, we putatively define HA-binding IgM/D$^-$CD38$^+$ B-cell population as memory-like B-cell population.

After pulmonary influenza virus infection, IgA-secreting plasma cells develop in the lung concomitantly with the presence of IgA Ab in bronchoalveolar lavage fluids (BALFs) (6, 18). To know the relative distribution of virus-specific IgA$^+$ B cells in lung and other organs, we compared the frequencies of IgA$^+$ cells among HA-binding IgM/D$^-$CD38$^+$ B cells in lung, MLN, and spleen. As expected, the memory-like B-cell population in lung expressed IgA isotype more frequently than the comparable populations in MLN and spleen; however, the average frequency of IgA$^+$ cells represented only 7% of the lung B-cell population (Fig. 1*C* and Fig. S3). The minor composition of IgA$^+$ cells among IgM/D$^-$ memory-like B cells in lungs is also supported by the previous estimation of IgA:IgG ratio (~1:10) in the precursors of plasma cells in lungs (6). This result suggests that IgA switching is enhanced but is not a major event during the development of the lung memory-like B-cell population following primary infection.

Memory-Like B-Cell Population in Lung Rapidly Differentiates into IgG- or IgA-Secreting Plasma Cells on Pulmonary Challenge. Accelerated responses to antigen challenge are a defining feature of memory B cells. To examine whether the memory-like B-cell population in lung are indeed responding to secondary infection, we detected lung B cells proliferating shortly after virus challenge by BrdU-incorporation assay. The memory-like B-cell population in the lungs did not incorporate detectable levels of BrdU at day 80 after primary infection (labeling period: 2 d) (Fig. 2*A*), consistent with the maintenance as a stable B-cell population in the absence of frequently dividing precursors. In contrast, by 2–3 d after secondary infection, BrdU$^+$ memory-like B-cell populations appeared in the lungs and MLNs, but not in the spleens (Fig. 2*A*). By day 4 postinfection, HA-binding IgM/D$^-$CD138$^+$ cells expressing plasmablasts/plasma cell markers accumulated in the lungs, and about half of these expressed IgA (Fig. 2*B*). ELISPOT analysis confirmed the prompt appearance of plasma cells in the lungs consisting of comparable frequencies of IgG- or IgA-secreting plasma cells (Fig. S4). These results suggest that, in response to virus reinfection, the memory-like B-cell population in lung divided and developed into plasma cells. In addition, regardless of infrequent expression of surface IgA on the memory-like B-cell populations, HA-binding class-switched plasma cells expressed IgG or IgA isotypes at similar frequencies following secondary challenge.

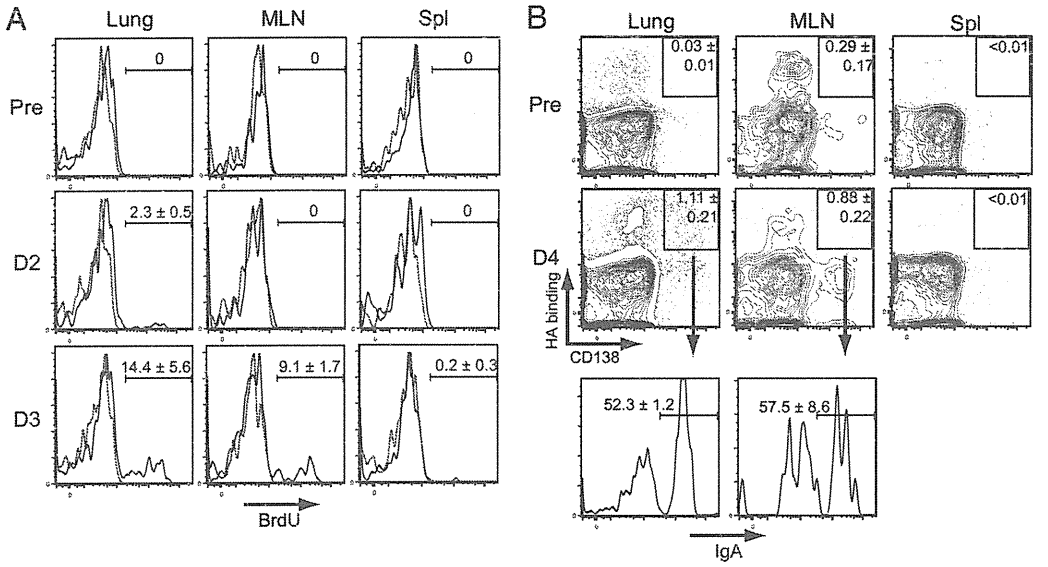

Fig. 2. Reactivation and terminal differentiation of the memory-like B-cell population in lung following secondary infection. (*A*) BALB/c mice were infected twice, with an 80-d interval. Mice were treated intraperitoneally with 1 mg BrdU for 48 h before analysis, and cells from the indicated organs were subjected to intracellular analysis for BrdU. Representative flow data for BrdU staining of HA-binding IgM/D$^-$CD38$^+$ B cells are presented (n = 3). (*B*) HA-binding/CD138 expression among B220^{dull}dump$^-$ cells and IgA expression among HA-binding CD138$^+$ cells are presented (n = 3–5).

Protective Function of the Memory-Like B-Cell Population in Lung. To examine the protective capacity of the memory-like B-cell population against reinfection, HA-binding IgM/D$^-$CD38$^+$ B cells were highly purified from the lungs and spleens of the mice >2 mo after primary infection, and then transferred into *scid* mice together with CD4$^+$ T cells isolated from the same donors. MLNs provided too few cells for adoptive transfer experiments and were not used. Accumulating evidence indicates that iBALT serves not only a site for initiating respiratory immune responses but also as a homing site for plasma cells (18, 19). Therefore, we considered that preforming iBALT structure might be required for reconstitution of local, secondary Ab responses to virus infection in adoptive hosts. To generate iBALTs in recipient mice before memory B-cell transfer, recipient *scid* mice were subjected to intranasal CpG treatment and i.v. transfer of spleen cells. As expected, this treatment generated peribronchial B-cell clusters 10 d later (Fig. 3 *A* and *B*). The treated mice were inoculated with challenging viruses 1 d after transfer of purified HA-binding IgM/D$^-$CD38$^+$ B cells (Fig. 3*C*), and then we determined virus titers in BALFs 6 d after infection. Remarkably, the mice reconstituted with the memory-like B-cell population in lung significantly reduced virus titers in BALFs, whereas those given splenic counterparts were similar to controls (Fig. 3*D*). Moreover, the protective ability of lung memory-like B-cell population was not observed in recipient mice without pre-CpG treatment (Fig. 3*E*).

To address whether adoptive transfer of the memory-like B-cell population in lung accelerated the Ab production in the respiratory tract, the numbers of HA-binding lung plasma cells and the levels of anti-HA Abs in BALFs were evaluated at the same time point. Adoptive transfer of lung memory-like B-cell population generated sixfold more IgG- and IgA-secreting plasma cells in the lungs compared with splenic counterparts in a manner depending on pre-CpG treatment of recipient mice (Fig. 3 *F* and *G*). Consistent with the results in secondary challenged BALB/c mice, the frequencies of IgA-secreting plasma cells were comparable to those of IgG-secreting plasma cells. These results support the contention that the enhanced IgA response following secondary infection reflects the increased supply of IgA-secreting plasma cells from memory and not naïve B cells. In accordance with ELISPOT data, anti-HA IgG and IgA Ab titers in BALFs were elevated in the mice reconstituted with the lung B-cell population after CpG treatment but not in those given the splenic B-cell population (Fig. 3*H*). Together, these data indicate that HA-binding IgM/D$^-$CD38$^+$ lung B cells are able to generate large amounts of Abs at the site of virus replication to confer protection more effectively than splenic counterparts. Moreover, given the successful reconstitution of local, secondary Ab responses in adoptive hosts, we conclude that HA-binding IgM/D$^-$CD38$^+$ B cells represent memory B cells in both phenotypes and functions.

Protective Functions of IgG Versus IgA Abs in Respiratory Tracts. Although it is established that secretory IgA can provide protection more effectively than IgG in upper respiratory tracts (20, 21), it is not known whether IgA in lower respiratory tracts contributes to protection in the presence of IgG. To estimate the contribution of IgG and IgA Abs in BALFs to virus neutralization, we first determined the titers of HA-binding IgG and IgA Abs. Consistent with comparable accumulation of IgG- and IgA-secreting plasma cells in the lungs (Figs. 2 and 3), BALFs in secondary challenged mice contained both HA-binding IgG and IgA Abs (Fig. 4*A*). The relative contributions of IgG and IgA to virus neutralization were estimated using BALFs depleted of either IgG or IgA Abs by affinity chromatography. We observed that removal of either IgG or IgA reduced virus-neutralizing activity of BALFs by two- to threefold (Fig. 4*B*), indicating partial, but not complete, reduction in activity. Moreover, removal of both IgG and IgA reduced virus-neutralizing activity to levels close to the detection limit. These data suggest that concomitant production of IgG and IgA Abs is required to achieve maximum neutralization activity.

Virus Particles Enhance Secondary IgA Response by Recruiting IgA-Secreting Plasma Cells from IgA$^-$ Memory B Cells. To explore the mechanisms for enhanced IgA secretion following secondary infection, we first examined whether the enhanced IgA response depends on intranasal infection by live viruses. Similar to Fig. 3, *scid* mice were reconstituted with either lung or splenic memory B cells and then subjected to i.p. boosting with formalin-inactivated

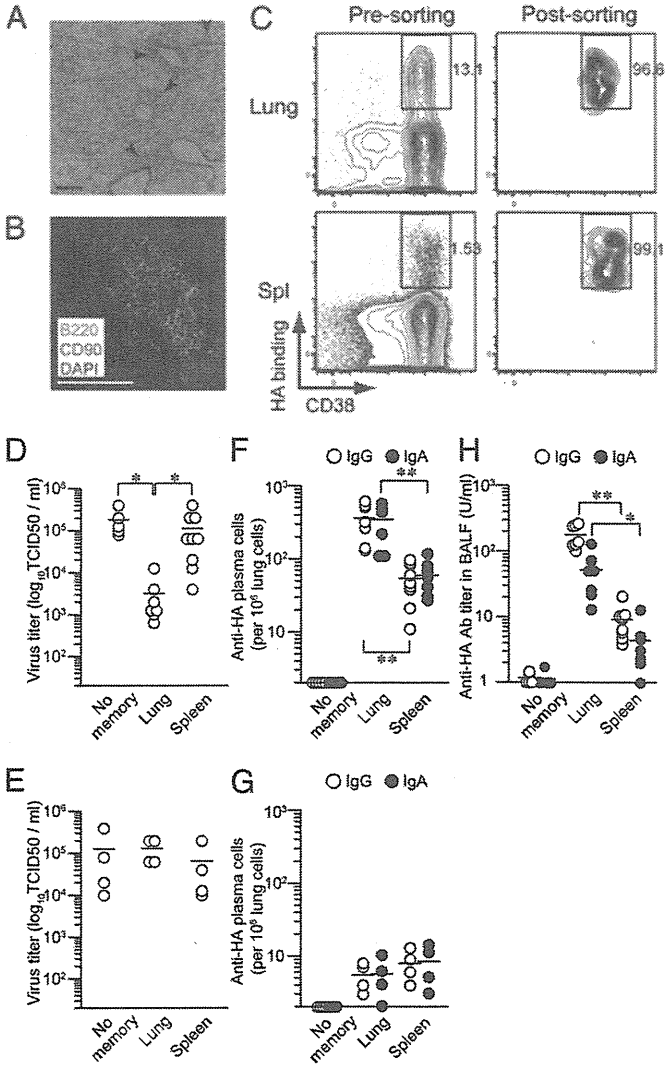

Fig. 3. Protective function of the memory-like B-cell population against secondary infection. (*A*) CB17-*scid* mice were injected intranasally with CpG and i.v. with BALB/c splenocytes. Ten days after treatment, lung sections were stained with HE (*A*) or B220 (green), CD90 (red), and DAPI (blue) (*B*). A representative section (n = 6) is presented. Arrowheads indicate iBALT-like structures. (Scale bar: 500 μm in *A* and 100 μm in *B*). (*C*) HA-binding IgM/D$^-$CD38$^+$ B cells were sorted from pooled lungs and spleens (n = 10). (*D* and *E*) CpG-treated (*D*) or untreated (*E*) CB17-*scid* mice were reconstituted with either lung or splenic memory-like B-cell population (3,000 cells per mouse) together with splenic B cells from naïve mice and CD4$^+$ T cells from infected mice. Splenic naïve B cells were added to prevent the loss of small numbers of memory-like B-cell population after sorting. On day 6 postinfection, virus titers in BALFs were determined. (*F* and *G*) HA-binding IgG and IgA-secreting plasma cells in the lungs of CpG-treated (*F*) or untreated (*G*) mice were enumerated by ELISPOT. (*H*) HA-binding IgG and IgA Ab titers in BALFs of CpG-treated mice were estimated by ELISA. In *D–H*, each circle represents the result for an individual mouse. *P < 0.05; **P < 0.01.

viruses, which are defective in replication but retain structure of virus particles. Reactivated lung memory B cells generated IgA-secreting plasma cells at increased frequencies of 40% among class-switched plasma cells (Fig. 5*A* and *B*). Although the numbers were lower than those of lung memory B cells, reactivated splenic memory B cells also increased the frequencies of IgA-plasma cells upon secondary challenge (Figs. 1*C* and 5*B*; 2.2 ± 1.0% (n = 4) vs. 12.1 ± 5.4% (n = 4), P < 0.05). These data indicate that enhanced IgA secretion from restimulated memory B cells does not require live virus infection or a mucosal environment.

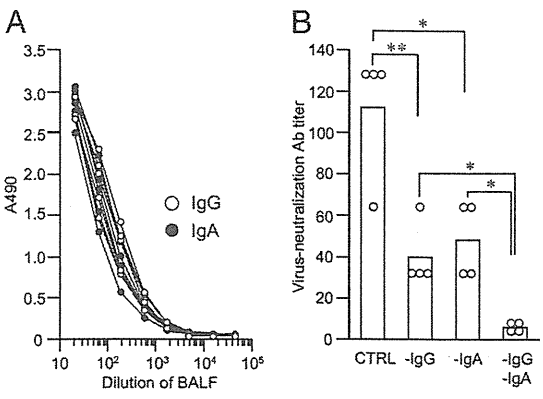

Fig. 4. Relative contribution of IgG and IgA Abs in BALFs to virus-neutralization. (*A*) Seven days after secondary challenge of BALB/c mice, anti-HA IgG and IgA Ab titers in BALFs were detected by ELISA. Each line represents the result for an individual mouse. (*B*) Virus-neutralization Ab titers in BALFs were determined by in vitro assay using MDCK cells. In *B*, each circle represents the result for an individual mouse. *P < 0.05; **P < 0.01.

To examine how virus particles enhance IgA responses of restimulated memory B cells, HA-binding IgA$^+$ and IgA$^-$ memory B cells in the lungs were separately transferred into recipient mice at 200 cells per mouse (Fig. 5*C*). Single-cell RT-PCR analysis revealed that only 2.1% of sorted IgA$^-$ population express J_H-Cα mRNA (Fig. S5). The reactivated lung IgA$^-$ memory B cells generated both IgG- and IgA-secreting plasma cells approximately at a ratio of 3:1 (Fig. 5*D*), suggesting the recruitment of IgA-secreting plasma cells from IgA$^-$ memory B cells after secondary stimulation with virus particles. Moreover, IgA production through IgA$^-$ memory B cells required the restimulation with virus particles, as rHA proteins could not elicit IgA-secreting plasma cells from IgA$^-$ memory B cells, whereas IgG-secreting plasma cells were comparably generated (Fig. 5*E*). Together, these data show that secondary IgA production is enhanced by recruitment of IgA-secreting plasma cells from IgA$^-$ memory B cells in a manner dependent on virus particles.

Discussion

Here, we have demonstrated that infected lungs harbor antigen-specific, class-switched B cells expressing CD38, CD73, CD80, and CD273, which are the most reliable surrogate markers for murine memory B cells. Moreover, two lines of evidences support that they promptly differentiate into mature plasma cells upon reinfection. First, lung memory B cells started to proliferate on day 2 after reinfection, when memory B cells in MLNs and spleens were still inert (Fig. 2*A*). Second, transferred lung memory B cells were able to generate IgG and IgA-secreting plasma cells in the lungs of adopted hosts after reinfection. Together, we conclude that antigen-specific memory B cells localize and respond to antigenic challenge in the lungs following pulmonary influenza virus infection.

The most striking feature of lung memory B cells is their ability to reduce virus spread in lower respiratory tracts of recipient mice. Given that lung memory B cells provided local IgG and IgA Ab in recipient mice following virus challenge, it is conceivable that both isotypes contribute to virus neutralization in situ. This idea is supported by the fact that virus neutralization depends on both IgG and IgA Abs in vitro (Fig. 4). Dispensability of IgA for providing protection in the lower respiratory tracts was previously suggested as vaccinated, IgA-deficient mice were found to be fully resistant to pulmonary influenza virus infection (22). However, IgA-deficient mice might use compensatory mechanisms that lead to altered expression of other Ab isotypes (23, 24). Given that systemic injection of anti-HA IgA

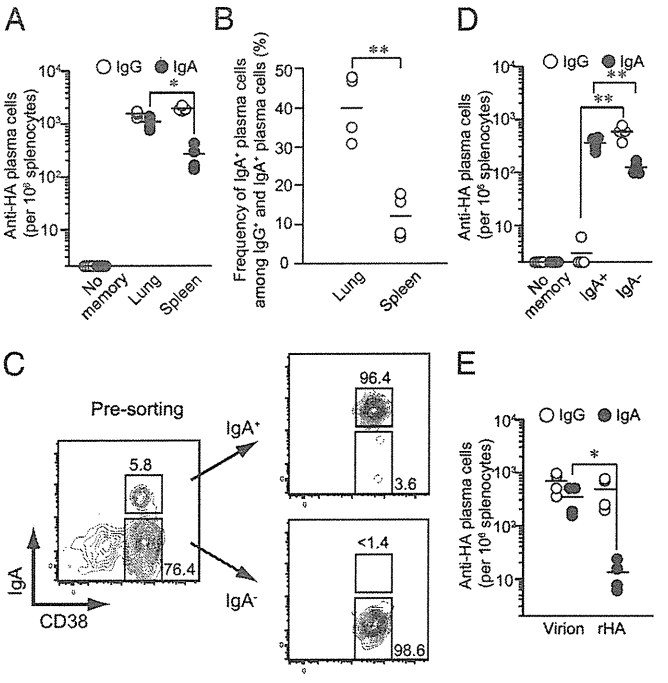

Fig. 5. Virus-dependent recruitment of IgA-secreting plasma cells from IgA$^-$ memory B cells. (*A*) CB17-*scid* mice were reconstituted similarly to Fig. 3*D* and boosted with inactivated viruses. At day 7 after boosting, the numbers of HA-binding IgG$^+$ and IgA$^+$ plasma cells were enumerated and plotted. (*B*) The frequencies of IgA$^+$ plasma cells among IgG$^+$/IgA$^+$ plasma cells are shown. (*C*) IgA$^+$ and IgA$^-$ memory B cells were sorted from pooled lung cells and splenocytes (n = 10). (*D*) The recipient mice were reconstituted with 200 IgA$^+$ or IgA$^-$ memory B cells in the lungs together with B cells and CD4$^+$ T cells, and the numbers of IgG$^+$ and IgA$^+$ plasma cells were determined after boosting. (*E*) Mice were reconstituted with IgA$^-$ memory B cells in the lungs, and the numbers of IgG$^+$ and IgA$^+$ plasma cells were determined after boosting with inactivated viruses or rHA. In *A*, *B*, *D*, and *E*, each circle represents the result for an individual recipient mouse. *P < 0.05; **P < 0.01.

mAbs was effective to prevent the initial infection in lung airways (25), we prefer the idea that both IgG and IgA Abs in lung airways contribute to virus neutralization.

The mechanism underlying the ability of lung memory B cells to supply local IgG and IgA Abs remains an important question to be addressed. Lung memory B cells express CD69 and CXCR3, possible mediators of lung localization. Thus, one possibility is that transferred lung memory B cells home back to the lung, wherein they could generate IgG- and IgA-secreting plasma cells at virus replication sites. This possibility is supported by requirement for intranasal CpG treatment before memory B-cell transfer. CpG-induced inflammation would trigger the local expression of several ligands (e.g., CXCL9 and CXCL10) for chemokine and/or homing receptors expressed on lung memory B cells. However, without pre-CpG treatment, the reduction of virus spread was not observed in the mice reconstituted with lung memory B cells (Fig. 3 *D*–*G*). The alternative possibility is that transferred lung memory B cells home to the MLNs, where they supply plasma cells in the lungs upon reinfection. Although we made tremendous efforts for in vivo tracing of transferred memory B cells, our attempts were unsuccessful due to a paucity of memory B cells.

B-cell intrinsic recognition of intact viruses is often hampered by the tissue tropisms of virus replication in nonlymphoid organs. Following pulmonary influenza virus infection, lung localization of memory B cells is one way to facilitate B cell intrinsic recognition for shaping the magnitude and quality of protective effector functions. Better understanding of the generation, maintenance, and reactivation of memory B cells in lung provides important insights for the development of vaccines for protection against influenza virus and other respiratory pathogens.

Materials and Methods

Mice and Viruses. Mice and viruses used in this study are described in *SI Materials and Methods*.

Cell Preparation and Flow Cytometry. Lung cells were isolated by Percoll gradient centrifugation after digestion with collagenase D and DNase I. Single-cell suspensions from lungs, MLNs, and spleens were stained with mixtures of biotinylated mAbs, followed by fluorescence-conjugated mAbs. BrdU-labeled cells were detected by using BrdU Flow kit (BD Biosciences). Stained cells were analyzed or purified using FACS Canto II or FACS Aria (BD Bioscience). Detailed methods are included in *SI Materials and Methods*.

Quantification of Anti-HA Abs and Plasma Cells. HA-binding Abs and plasma cells were quantified by ELISA and ELISPOT using rHA as coating antigens and anti-mouse IgG- or IgA Abs as secondary Abs. Virus-neutralization Ab titers were quantified by microneutralization assay using MDCK cells and X31 virus (100 $TCID_{50}$) (26). Detailed methods are included in *SI Materials and Methods*.

Statistical Analyses of Data. Statistical significance was determined by an unpaired two-tailed Student t test. $P < 0.05$ were considered significant.

ACKNOWLEDGMENTS. We thank Dr. G. Kelsoe (Duke University) for critical reading of the manuscript; Dr. T. Tsubata (Tokyo Medical and Dental University) for providing the X31 virus; and Ms. E. Watanabe, E. Izumiyama, and K. Fukuhara for technical assistance. This study was supported by grants from the Ministry of Education, Culture, Sports, Science, and Technology in Japan (to Y.T. and T.K.), the Japan Science and Technology Agency, Core Research for Evolutional Science and Technology (to Y.T. and T.K.); and the Emerging and Re-Emerging Infectious Diseases and Regulatory Science of Pharmaceuticals and Medical Devices of the Ministry of Health, Labour and Welfare in Japan (to Y.T. and K.K.).

1. Dörner T, Radbruch A (2007) Antibodies and B cell memory in viral immunity. *Immunity* 27:384–392.
2. Sallusto F, Lanzavecchia A, Araki K, Ahmed R (2010) From vaccines to memory and back. *Immunity* 33:451–463.
3. Coro ES, Chang WL, Baumgarth N (2006) Type I IFN receptor signals directly stimulate local B cells early following influenza virus infection. *J Immunol* 176:4343–4351.
4. Moyron-Quiroz JE, et al. (2004) Role of inducible bronchus associated lymphoid tissue (iBALT) in respiratory immunity. *Nat Med* 10:927–934.
5. Jones PD, Ada GL (1987) Persistence of influenza virus-specific antibody-secreting cells and B cell memory after primary murine influenza virus infection. *Cell Immunol* 109: 53–64.
6. Joo HM, He Y, Sangster MY (2008) Broad dispersion and lung localization of virus-specific memory B cells induced by influenza pneumonia. *Proc Natl Acad Sci USA* 105: 3485–3490.
7. Baumgarth N, et al. (1999) Innate and acquired humoral immunities to influenza virus are mediated by distinct arms of the immune system. *Proc Natl Acad Sci USA* 96: 2250–2255.
8. Ridderstad A, Tarlinton DM (1998) Kinetics of establishing the memory B cell population as revealed by CD38 expression. *J Immunol* 160:4688–4695.
9. Takahashi Y, Ohta H, Takemori T (2001) Fas is required for clonal selection in germinal centers and the subsequent establishment of the memory B cell repertoire. *Immunity* 14:181–192.
10. Bachmann MF, Odermatt B, Hengartner H, Zinkernagel RM (1996) Induction of long-lived germinal centers associated with persisting antigen after viral infection. *J Exp Med* 183:2259–2269.
11. Rothaeusler K, Baumgarth N (2010) B cell fate decisions following influenza virus infection. *Eur J Immunol* 40:366–377.
12. Bhattacharya D, et al. (2007) Transcriptional profiling of antigen-dependent murine B cell differentiation and memory formation. *J Immunol* 179:6808–6819.
13. Tomayko MM, et al. (2008) Systematic comparison of gene expression between murine memory and naive B cells demonstrates that memory B cells have unique signaling capabilities. *J Immunol* 181:27–38.
14. Anderson SM, Tomayko MM, Ahuja A, Haberman AM, Shlomchik MJ (2007) New markers for murine memory B cells that define mutated and unmutated subsets. *J Exp Med* 204:2103–2114.
15. Tomayko MM, Steinel NC, Anderson SM, Shlomchik MJ (2010) Cutting edge: Hierarchy of maturity of murine memory B cell subsets. *J Immunol* 185:7146–7150.
16. Kohlmeier JE, et al. (2009) CXCR3 directs antigen-specific effector CD4+ T cell migration to the lung during parainfluenza virus infection. *J Immunol* 183:4378–4384.

17. Lee YT, et al. (2011) Environmental and antigen receptor-derived signals support sustained surveillance of the lungs by pathogen-specific cytotoxic T lymphocytes. *J Virol* 85:4085–4094.
18. GeurtsvanKessel CH, et al. (2009) Dendritic cells are crucial for maintenance of tertiary lymphoid structures in the lung of influenza virus-infected mice. *J Exp Med* 206: 2339–2349.
19. Halle S, et al. (2009) Induced bronchus-associated lymphoid tissue serves as a general priming site for T cells and is maintained by dendritic cells. *J Exp Med* 206: 2593–2601.
20. Renegar KB, Small PA, Jr. (1991) Passive transfer of local immunity to influenza virus infection by IgA antibody. *J Immunol* 146:1972–1978.
21. Renegar KB, Small PA, Jr., Boykins LG, Wright PF (2004) Role of IgA versus IgG in the control of influenza viral infection in the murine respiratory tract. *J Immunol* 173: 1978–1986.
22. Mbawuike IN, et al. (1999) Mucosal immunity to influenza without IgA: an IgA knockout mouse model. *J Immunol* 162:2530–2537.
23. Harriman GR, et al. (1999) Targeted deletion of the IgA constant region in mice leads to IgA deficiency with alterations in expression of other Ig isotypes. *J Immunol* 162: 2521–2529.
24. Arulanandam BP, et al. (2001) IgA immunodeficiency leads to inadequate Th cell priming and increased susceptibility to influenza virus infection. *J Immunol* 166: 226–231.
25. Palladino G, Mozdzanowska K, Washko G, Gerhard W (1995) Virus-neutralizing antibodies of immunoglobulin G (IgG) but not of IgM or IgA isotypes can cure influenza virus pneumonia in SCID mice. *J Virol* 69:2075–2081.
26. Takahashi Y, et al. (2009) Protective immunity afforded by inactivated H5N1 (NIBRG-14) vaccine requires antibodies against both hemagglutinin and neuraminidase in mice. *J Infect Dis* 199:1629–1637.